ACS APPLIED MATERIALS & INTERFACES

Research Article

www.acsami.org

Conjugation of Dexamethasone to C60 for the Design of an Anti-Inflammatory Nanomedicine with Reduced Cellular Apoptosis

Yi Zhang,[†,§] Lu Wang,[†,§] Yanhong Sun,[*,†] Ying Zhu,[†] Zengtao Zhong,[*,‡] Jiye Shi,[†,∥] Chunhai Fan,[†] and Qing Huang[†]

[†]Laboratory of Physical Biology, Shanghai Institute of Applied Physics, Chinese Academy of Sciences, Shanghai 201800, China

[‡]College of Life Sciences, Nanjing Agricultural University, Nanjing 210095, China

[§]Universtiy of Chinese Academy of Sciences, Beijing 100049, China

[∥]UCB Pharma, 208 Bath Road, Slough SL1 3WE, U.K.

ABSTRACT: Dexamethasone (DEX) is a well-known anti-inflammatory drug, whose widespread clinical use is nevertheless restricted by its serious side effects. By conjugation of DEX with C_{60}, we found that this nanomedicine retained the anti-inflammatory activity of DEX while reducing side effects in the animal model. In mouse thymocytes, the CCK-8 assay showed that the cytotoxicity of DEX−C_{60} was significantly lower than that of free DEX. Flow cytometric studies revealed that incubation with DEX−C_{60} induced much less apoptotic thymocytes. Interestingly, such reduced cytotoxicity and apoptosis were not observed when equal moles of free C_{60} and free DEX were coincubated with thymocytes, suggesting that the conjugation alters the signal pathway of DEX. Indeed, we found that the binding of DEX−C_{60} and a glucocorticoid receptor (GR) was partially blocked in the thymocytes, which resulted in down-regulation of several apoptosis-related genes. These findings help understand the mechanism of beneficial effects of this new nanomedicine, DEX−C_{60}, and promote its clinical applications.

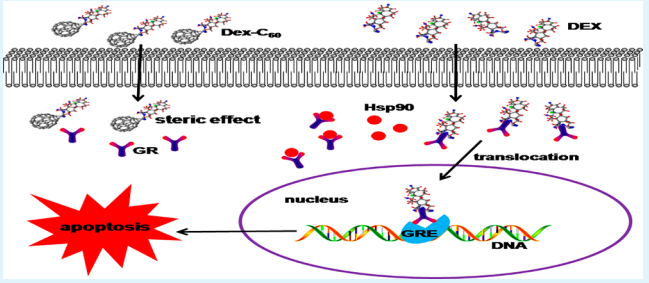

KEYWORDS: *dexamethasone, C_{60}, glucocorticoid receptor, apoptosis, thymocytes*

1. INTRODUCTION

Dexamethasone (DEX) is a synthetic glucocorticoid (GC) that is widely used to treat inflammatory and autoimmune diseases, including the inflammatory responses to cardiopulmonary bypass and acute infection.[1−5] Unfortunately, DEX is associated with potentially serious side effects, including gastrointestinal dysfunction, adrenal suppression, and hypersensitivity in the central nervous system.[6−9]

Until recently, the mechanisms underlying the anti-inflammatory activity and the side effect of DEX have remained unclear.[10−13] Nevertheless, it was demonstrated that DEX could induce apoptosis of many cell types, including mouse thymocytes.[14,15] DEX increases the intracellular production of reactive oxygen species (ROS), such as superoxide and hydrogen peroxide (H_2O_2), which increase oxidative stress.[16,17] ROS play important roles in apoptosis induction in physiologic and pathologic conditions.[18,19] Therefore, it is reasonable to think that the side effects of DEX are closely related to the generation of ROS.[20−22]

Many studies have showed that the anti-inflammatory properties and the side effects of DEX are associated with the glucocorticoid receptor (GR).[23−25] The GR is an intracellular receptor that is mainly located in the cytoplasm in association with heat shock proteins (HSPs) in its inactive form.[26−28] After binding to DEX, the DEX−GR complex translocates to the nucleus and binds to a glucocorticoid response element (GRE) and modulates the expression of target genes, including interleukin-6 and nuclear factor-κb.[29,30] It is generally believed that the binding of DEX to GR is involved in DEX-induced apoptosis.[31,32]

C_{60} is a carbon nanomaterial with many potential biological applications, including drug delivery, neuroprotection, and enzyme inhibition. One of the most important features of C_{60} is its ability to scavenge ROS, which makes it an excellent antioxidant in vitro. C_{60} was also reported to reduce H_2O_2-induced cytotoxicity, free radical formation, and mitochondrial damage.[33−35] Gharbi et al. reported that aqueous C_{60} suspensions could protect the rodent liver against free-radical-induced damage.[36] Similarly, Cai et al. reported C_{60} is a mitochondrial protective antioxidant with direct radical scavenging activity.[37] As ROS-induced apoptosis could be partly responsible for the side effects of DEX, it is reasonable to suggest that C_{60} could reduce the incidence of side effects. In our former study, we reported on the successful synthesis and characterization of DEX−C_{60}, a new C_{60} derivative. Our experiments confirmed that the anti-inflammatory properties of

Received: March 30, 2013
Accepted: May 13, 2013
Published: May 13, 2013

   dx.doi.org/10.1021/am401153k | ACS Appl. Mater. Interfaces 2013, 5, 5291−5297

DEX were retained when conjugated with C_{60}.[38] Furthermore, behavioral tests showed DEX−C_{60} did not affect central nervous system activity in mice, implying a low risk of side effects.[38] These earlier studies also highlighted the broad clinical applications of DEX−C_{60}.

In this paper, we determined the cytotoxicity of DEX−C_{60} in mouse thymocytes to identify the mechanism underlying its lower risk of side effects. We found that the reduction in thymocyte apoptosis associated with DEX−C_{60} was not related to the scavenging of ROS by C_{60}. Instead, in vivo and in vitro experiments showed reduced binding of DEX−C_{60} to GR, which reduced the activity of GRE and conferred lower cytotoxicity.

2. EXPERIMENTAL SECTION

2.1. Reagents and Instruments. C_{60} (99.9% purity), DEX, GR, and RU-486 were obtained from Sigma-Aldrich Co. Ltd. The Cell Counting Kit-8 (CCK-8) assay was purchased from Dojindo Co. Ltd. Anti-DEX and anti-GR antibodies were obtained from Abcam Co. Ltd. Fetal bovine serum, penicillin, and streptomycin are purchased from Invitrogen Corporation (Carlsbad, CA). APC-annexin V and 7-amino-actinomycin (7-AAD) were purchased from BD Biosciences Co. Ltd. (Shanghai, China). All other chemicals were purchased from Sinopharm Chemical Reagent Co. Ltd. (Shanghai, China).

2.2. Preparation and Characterization of the Dex-C_{60} Suspension. DEX−C_{60} was prepared as described by Liu et al.[38] C_{60} and DEX were dispersed in chloroform (18 mL), followed by the addition of dicyclohexyl carbodimide (22 mg, 107 μmol) and 4-dimethylaminopyridine (negligible amount) with gasification under N_2 for 5 min. The resulting mixture was stirred for 7 days in the dark at room temperature. Then DEX−C_{60} was purified by column chromatography with 8:2 $CH_3COOC_2H_5/CS_2$; the purified DEX−C_{60} was a brown solid. DEX−C_{60} was dissolved in water and suspended in polyvinylpyrrolidone (PVP) by mixing 115 μmol of DEX−C_{60} with 95 μmol of PVP in a quartz mortar. The mixture was milled until the color turned dark brown. Suspensions of C_{60} and DEX were also prepared. The distribution of particle diameter of C_{60} and DEX−C_{60} was analyzed by dynamic light scattering (DLS), and the ζ potential was used to analyze dispersion stability.

2.3. Preparation of RU-486 and DEX. RU-486 (8.27 mg) was added to 551 μL of dimethyl sulfoxide (DMSO), and 28.64 μL of the RU-486−DMSO suspension was mixed with 971 μL of RPMI-1640 medium. The final concentration of RU-486 was 500 μM.

DEX (56.29 mg) was dissolved in 56.29 mL of alcohol (100%), and the DEX−alcohol suspension was diluted with RPMI-1640 medium. The final concentration of DEX was 1 μM.

2.4. Thymocyte Preparation. All animal experiments were performed in accordance with guidelines from the local ethics committee. Female C57BL/6 mice (18−22 g) were obtained from Shanghai Experimental Animal Center. The animal room was maintained at 22 °C with lights on from 06:00 to 18:00. The mice were fed with a standard diet and were provided water. All animal experiments were reviewed and approved by the Institutional Animal Care and Use Committee.

The thymus from C57BL/6 mice was coated with ice-cold phosphate-buffered saline (PBS) and placed in a 60 mm culture dish. Single-cell suspensions were made by crushing the thymus through a cell strainer and filtering the suspension. The cell suspension was centrifuged at 500*g* for 3 min at 4 °C. The cells were then cultured for 6 h in RPMI-1640 medium under 5% CO_2, in an incubator maintained at 37 °C.

2.5. Analysis of Thymocytes. Cell viability was evaluated using the Cell Counting Kit-8 (CCK-8) assay. CCK-8 was just as WST-8 to produce formazan in the presence of an electron mediator, and the amount of the formazan generated in cells was directly proportional to the number of living cells. The thymocytes were seeded in 96-well plates at a density of 5×10^4 cells per well. DEX and DEX-C60 were previously dissolved in RPMI-1640 medium at different concentrations (2, 1.0, 0.5, 0.1, and 0.01 μM) and added into a 96-well plate. The thymocytes were incubated in the medium under 5% CO_2 in an incubator maintained at 37 °C for 6 h. Then, 10 μL of the CCK-8 was added to each well of a 96-well plate incubated for 2 h. The absorbance was measured at 450 nm using a microplate reader (Biorad model 550). Cell viability is expressed as a percentage of control.

Cell apoptosis was measured by flow cytometry. Cell samples were divided into 24-well plates, and the number of cells in each treatment groups is not less than 100 000. Annexin V-APC and 7-AAD were used as fluorescence agents. Cells are collected and washed three times with PBS and then incubated with 5 μL of annexin V-APC and 7-AAD for 15 min at 25 °C. Next, 200 μL of binding buffer was added to the staining solution, and apoptosis was analyzed by flow cytometry.

2.6. Enzyme-Linked Immunosorbent Assays (ELISAs). DEX−GR binding was measured with an ELISA using a monoclonal rabbit antimouse DEX antibody. First, 96-well plates were coated by incubation with 2 μg/mL of GR solution for 48 h. Then, the antibody was blocked with 1% bovine serum albumin/phosphate solution. The test samples were added to duplicate wells and incubated overnight after washing. DEX, DEX−C_{60}, and C_{60} were added to independent wells and incubated with GR overnight. After washing, the antibody (diluted 1:500) was added to each plate for 6 h at room temperature. The complex was detected using horseradish peroxidase-conjugated goat antirabbit IgG with absorbance measured at 405 nm.

2.7. RT-PCR. The cells were washed three times with PBS and were collected. Each cell sample was lysed in 1 mL of Trizol Reagent and 0.2 mL of chloroform. The cell suspensions were shaken vigorously for 15 s and incubated for 3 min at 25 °C. The suspensions were centrifuged at 12 000 rpm for 15 min. The aqueous supernatant was transferred to a new tube, and 0.5 mL of isopropyl alcohol was added. The tube was left at room temperature for 10 min to precipitate RNA. The resulting RNA was washed with 1 mL of 75% ethanol and dissolved in Rnase-free water. The RNA concentration was measured at 260 nm.

Next, the RNA samples were heated to 70 °C for 5 min followed by 37 °C for 1 h in 25 μL of reaction mixture containing 2 μg of RNA, 0.5 μg of oligo-dT, 0.5 mM of each dNTP, 200 U of Moloney murine leukemia virus reverse transcriptase, and 5 μL of 5× reaction buffer. All samples were stored at −70 °C. The following primers were used: GADPH, 5′-GGGAGCCAAAAGGGTCATCATCTC-3′ and 5′-CCATGCCAGTGAGCTTCCCGTTC-3′; TDAG8, 5′-AATG-GATGTGATCGGGAG-3′ and 5′-GAGATTATAGACTAA-GAGGTGGAG-3′; GR, 5′-AATGGGCAAAGGCGATAC-3′ and 5′-TTGGCTCTTCAGACCTTCC-3′; Txinp, 5′-TGGACGATGTG-GACGACTC-3′ and 5′-GGAAAGACAACGCCAGAAG-3′.

2.8. Confocal Microscopy. For confocal microscopy, thymocytes were grown on glass coverslips in 24-well plates in 1 mL of RPML-1640 medium containing 10% FBS. After incubating for 24 h at 37 °C in a humidified atmosphere of 95% air and 5% CO_2, the medium was replaced with 1 mL of fresh medium containing DEX and DEX−C_{60}, respectively, and cultured for 2 h. The medium was then removed and washed twice with warm PBS and fixed in 4% paraformaldehyde with 4% sucrose for 30 min. Then, 3% bovine serum albumin and 0.2% Triton X-100 in PBS were added for 20 min. After washing twice with PBS, the cells were incubated with rabbit anti-GR antibody (1:1000) for 6 h, washed three times with PBS, and incubated with fluorescein isothiocyanate (FITC)-labeled goat antirabbit IgG for 1 h to stain nuclei. Cells were excited with a laser at 405 and 488 nm excitation.

2.9. Statistical Analysis. All of the variables were compared using one-way analysis of variance using GraphPad Prism version 5.0 for Windows. Differences are considered statistically significant for $p < 0.05$(*).

3. RESULTS AND DISCUSSION

3.1. Characteristics of the DEX−C_{60}, DEX, and C_{60} Suspensions. The DEX−C_{60} complex was synthesized according to the method of Liu et al.[38] The infrared and nuclear magnetic resonance spectra of the conjugate were consistent with those reported in prior studies.[33,38] In cell

culture experiments, we determined the distribution of particle diameters and ζ-potential of C_{60} and DEX−C_{60} in RPMI-1640. DLS was used to measure the mean distribution of particle diameters of DEX−C_{60}, and >80% of DEX−C_{60} nanoparticles were 155−300 nm in diameter. The major distribution of particle diameters of C_{60} was 167.9 nm, and that of DEX−C_{60} was 213.4 nm (Figure 1a,b). The ζ-potential of C_{60} was −2.5 mV, and the ζ-potential of DEX−C_{60} was −7.9 mV(Figure 1c,d). These results indicated that the DEX−C_{60} complex was synthesized successfully. After the DEX−C_{60} nanoparticles were incubated with RPMI-1640 for 1 week, no megascopic aggregation of DEX−C_{60} was observed in a previous study. Although DEX−C_{60} was stable in RPMI-1640 medium, DEX−C_{60} appeared to aggregate after storage for 30 days at 4 °C. The color of the DEX−C_{60} suspension turned brown, and peaks corresponding to DEX−C_{60} (596.9 nm in diameter) were detected by DLS. In our experiments, DEX−C_{60} was used to incubate with cells as soon as it was prepared, and the dispersion of DEX−C_{60} was perfect.

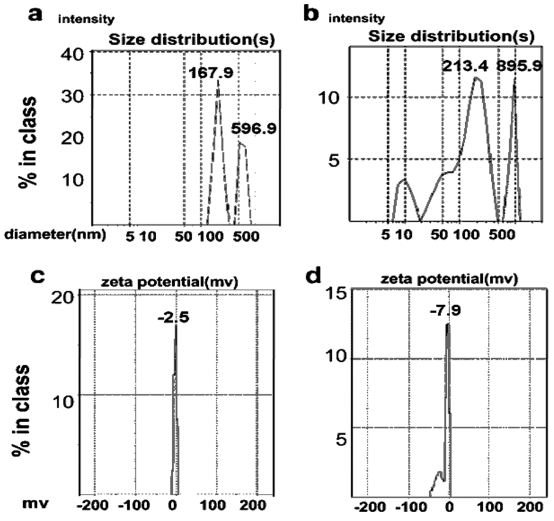

Figure 1. Characteristics of the C_{60} and DEX−C_{60} suspensions in different phases. (a) Distribution of particle diameters of C_{60}. (b) Distribution of particle diameters of DEX−C_{60}. (c) ζ-potential of C_{60}. (d) ζ-potential of DEX−C_{60}.

3.2. Cytotoxic and Apoptotic Effects by DEX−C_{60}. Although previous studies showed that DEX−C_{60} was associated with fewer side effects than DEX in an animal model, the underlying mechanism remained unknown. Here, we used mouse thymocytes as a cell model to compare the cytotoxic and apoptotic effects of DEX−C_{60} and DEX. DEX−C_{60} and DEX were separately dissolved in RPMI-1640 medium, and the concentrations of them were at gradient. Thymocytes were exposed to DEX−C_{60} or DEX at concentrations of 2, 1.0, 0.5, 0.1, and 0.01 μM (Figure 2a). Results of the CCK-8 assay indicated that DEX−C_{60} and DEX had dose-dependent cytotoxic effects on thymocytes. However, the cytotoxicity of DEX was greater than that of DEX−C_{60} at the same concentration. For example, following exposure to 0.01 or 0.1 μM DEX, 40% and 63% of cells died. By contrast, only about 50% of cells died when thymocytes were incubated with 1 μM DEX−C_{60}. Even when the DEX−C_{60} concentration was increased to 2 μM, more than 40% cells were still alive. These results clearly indicated that the cytotoxicity of DEX−C_{60} was much weaker than that of DEX.

In previous studies, including the study by Liu et al.,[38] C_{60} was used as an effective ROS scavenger. If C_{60} in DEX−C_{60} also protects against free radicals induced by DEX, coincubation of thymocytes with C_{60} may attenuate the reduction in viability caused by DEX. To test this hypothesis, thymocytes were pretreated with 50, 10, or 2 μM C_{60} followed by incubation with 100 nM DEX for 6 h. Cell viability was then determined using the CCK-8 kit. Interestingly, there were no significant differences of thymocyte viability between C_{60}-pretreated cells at any concentration as compared with cells without C_{60} pretreatment as >60% of the thymocytes in each group had died after 6 h of culture (Figure 2b). These results indicated that C_{60} itself will not reduce DEX-induced cytotoxicity and that a reduction of ROS did not explain the reduced cytotoxicity of DEX−C_{60}.

Wyllie et al. reported that DEX induces cellular apoptosis, which might be involved in its side effects.[39] Therefore, we determined the effects of C_{60}, C_{60} and DEX, and DEX−C_{60} on thymocyte apoptosis by flow cytometry (Figure 3). In a control group, the apoptotic rate of normal thymocytes was 5 ± 1.2%.

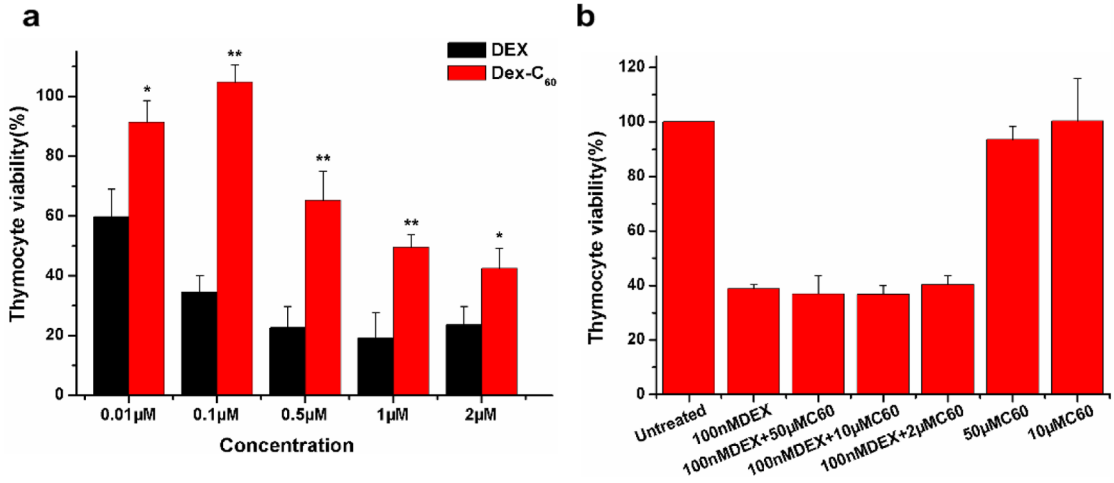

Figure 2. Viability of thymocytes treated with DEX or DEX−C_{60}. (a) Viability of thymocytes treated with DEX−C_{60} or DEX at the indicated concentrations. (b) Effects of C_{60} pretreatment on thymocyte viability.

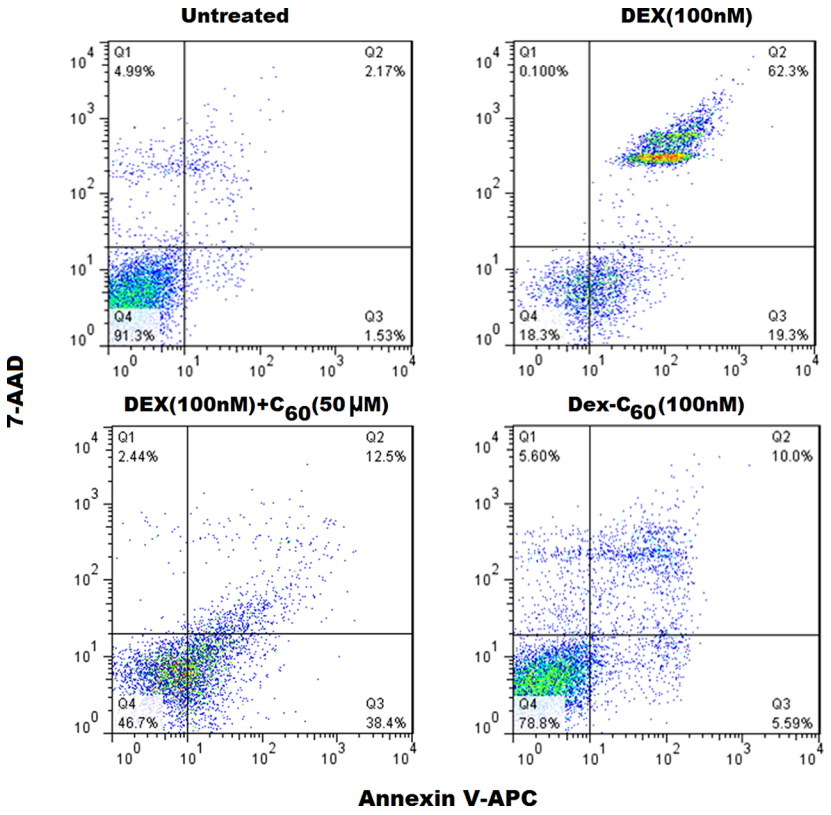

Figure 3. Results of flow cytometry after labeling cells with annexin V-APC and 7-AAD.

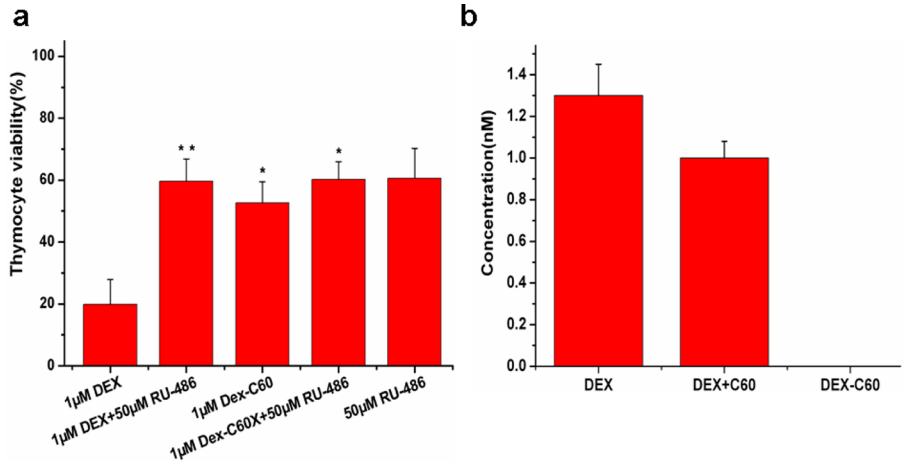

Figure 4. Results of the DEX−GR binding assay. (a) RU-486 suppressed GR binding activity. (b) GR binding activity following incubation with DEX, DEX and C_{60}, or DEX−C_{60}.

The apoptotic rate of thymocytes incubated with 100 nM DEX for 6 h was about 80%. DEX−C_{60} was associated with a low apoptotic rate of about 16%, consistent with the lower cytotoxicity of DEX−C_{60} compared with DEX. Interestingly, in cells pretreated with 50 μM C_{60}, over 50% of cells were apoptotic, indicating that C_{60} itself does not reduce the cytotoxicity of DEX. The results of flow cytometry were very consistent with those of viability tests. Accordingly, it seems likely that the low cytotoxicity of the DEX−C_{60} is not due to the free radical scavenging activity of C_{60}.

3.3. Effects of DEX−C_{60} on DEX−GR Binding. It was previously reported that DEX-induced apoptosis was related to the activity of the GR, a cytoplasmic receptor. After binding with DEX, the DEX−GR complex translocates from the cytoplasm to the nucleus[26,34,40] where it activate apoptosis signaling pathways.[41] As DEX−C_{60} was associated with reduced thymocyte apoptosis compared with DEX alone, we hypothesized that the complex may interfere with binding and translocation of the DEX−GR complex.

RU-486 is a potent GC antagonist that is used to block the GR in vitro and in vivo.[42] In our experiments, pretreatment of thymocytes with 50 μM RU-486 for 1 h prevented the loss of thymocyte viability caused by DEX, which was consistent with the results of earlier studies. However, pretreatment with RU-486 did not significantly affect the viability of cells treated with DEX−C_{60} (Figure 4a). These results suggest that DEX−C_{60} may improve viability through a mechanism similar to RU-486, by interfering with DEX−C_{60} binding to the GR.

dx.doi.org/10.1021/am401153k | ACS Appl. Mater. Interfaces 2013, 5, 5291−5297

To examine the binding between the GR and DEX−C_{60}, we performed ELISAs. Briefly, GR was coated onto the surface of 96-well plates, which was followed by the addition of DEX and DEX−C_{60}. After incubation overnight and washing, we added a DEX antibody to label DEX or DEX−C_{60} that was still bound to the GR. The results of this assay showed that there was no DEX−C_{60} bound to GR on the plate, whereas DEX was easily detected (Figure 4b). These data confirmed that DEX−C_{60} lost the ability to bind to GR. By contrast, DEX was detected in wells that were coincubated with DEX and C_{60}.

After DEX is taken up by cells, it binds to cytoplasmic GR, which is translocated to the nucleus, where it activates the transcription of downstream target genes.[42,43] Therefore, we performed immunostaining to determine the expression and localization of GR in cells treated with DEX−C_{60} or DEX. To visualize the GR, we stained cells with rabbit anti-GR antibody and FITC-labeled goat antirabbit IgG. As illustrated in Figure 5,

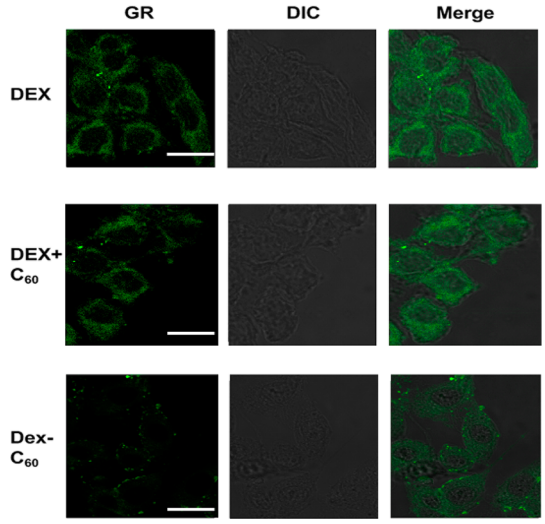

Figure 5. Effects of DEX−C60, DEX, and DEX and C60 on GR translocation in thymocytes. Scale bar = 20 μm.

the green fluorescent signal corresponding to FITC-labeled GR was detected in the cytoplasm and nucleus of cells treated with DEX, which was consistent with the results of previous studies. Treatment with DEX−C_{60} was associated with a much weaker signal for GR in the cytoplasm, indicating reduced GR expression. Furthermore, the signal for GR was negligible in the nucleus, which indicates the absence of GR translocation. These results provide in vitro evidence that DEX−C_{60} hardly bound to the GR. Meanwhile, the expression and translocation of GR in thymocytes coincubated with C_{60} and DEX was not significantly different from that in cells incubated with DEX alone. These results provide further confirmation that C_{60} itself does not reduce the cytotoxicity of DEX because it did not inhibit DEX−GR binding or receptor translocation.

3.4. Effects of the DEX−C_{60} Complex on DEX-Induced Expression of Apoptosis-Related Genes. The proapoptotic effects of DEX involve GR-mediated activation of downstream genes, including genes involved in the mitochondrial apoptotic pathway. The DEX−GR complex binds to the GREs on its target genes and modulates their transcription.[44−46] Studies using mice expressing a dimerization-deficient GR mutant indicate that GC-induced thymocyte apoptosis requires the gene transactivation function of this receptor.[47] T cell death-associated gene 8 (TDAG8) is a G-protein-coupled receptor that is transcriptionally upregulated by DEX and overexpressed in DEX-induced apoptosis. TDAG8 was first identified by differential mRNA display during thymocyte apoptosis induced by T-cell receptor (TCR) engagement.[48] Recent studies have shown that TDAG8 expression was positively correlated with thymocyte apoptosis. Thioredoxin-interacting protein (TXNIP) is a regulator of metabolism and an inhibitor of the antioxidant thioredoxin and could mediate DEX-induced apoptosis.[49] The expression levels of these genes were also associated with caspase-3 activity and DEX-induced cell apoptosis.

In this study, we determined the gene expression levels of GR, TDAG8, and TXNIP by RT-PCR. As shown in Figure 6, the mRNA expression levels of TDAG8 and TXNIP in DEX-treated cells were 6-fold and 2-fold higher, respectively, than those in untreated cells. GR gene expression was also increased slightly in DEX-treated cells. Conversely, in cells treated with DEX−C_{60}, the mRNA expression levels of these genes were significantly lower than those in DEX-treated cells. These results indicate that DEX−C_{60} inhibits DEX-induced expression of apoptosis-related genes, probably because the binding of this component to GR is reduced, thus preventing GR translocation and GR-mediated expression of TDAG8 and TXNIP. Consequently, this treatment attenuated the side effects of DEX, providing a novel method to reduce the side effects of DEX therapy.

The data presented in this paper provide compelling evidence that the C_{60} component of the DEX−C_{60} complex has a steric effect by blocking binding of DEX to GR. We found that DEX−C_{60} is readily taken by thymocytes but fails to bind

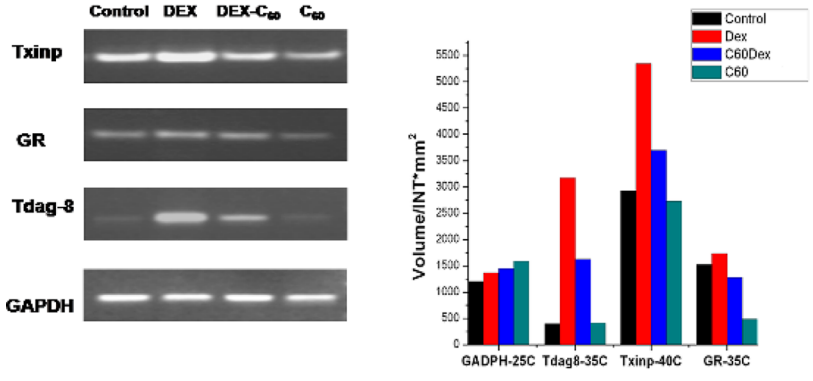

Figure 6. RT-PCR analysis of TDAG8, TXNIP, and GR mRNA expression.

dx.doi.org/10.1021/am401153k | ACS Appl. Mater. Interfaces 2013, 5, 5291−5297

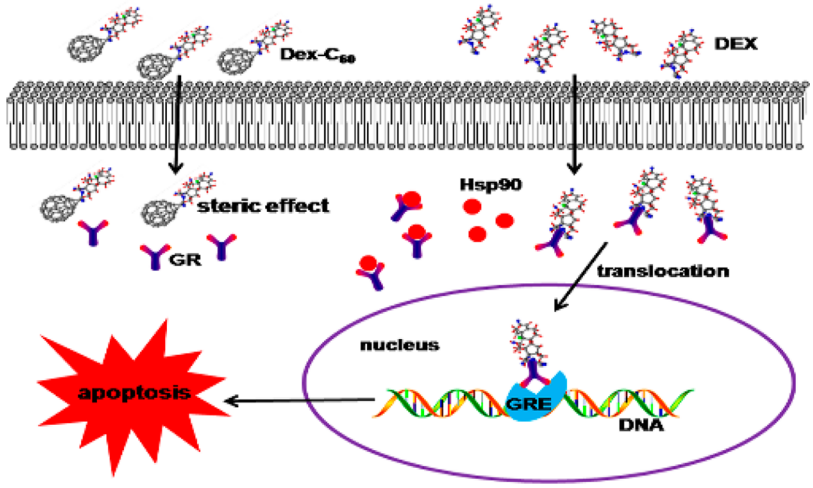

Figure 7. Steric effects of C_{60} in the DEX−C_{60} complex on DEX−GR binding and GR activity. Following binding of GCs to GR, the GC−GR complex translocates from the cytoplasm into the nucleus via an endogenous nuclear transport machinery. In cells treated with DEX−C_{60}, the C60 component had a steric effect that blocked interactions between the DEX component and the GR.

to GR, which prevents GR translocation to the nucleus. Consequently, GR is unable to activate the transcription of apoptosis-related genes. This pathway is illustrated in Figure 7.

4. CONCLUSIONS

In conclusion, we found that GR in thymocytes did not successfully bind to the DEX component of the DEX−C_{60} complex, preventing its translocation into the nucleus. Thus, treatment with the DEX−C_{60} complex prevented transcription of the downstream targets of the GR, including those in the apoptotic pathway. These findings help to explain the lower incidence of side effect of DEX−C_{60} compared with DEX alone. Ultimately, we provide evidence that a nanoparticle could inhibit the binding between a bioactive molecule and its receptor when the molecule is conjugated to a nanoparticle, as the complex was unable to approach the receptor because of steric hindrance caused by the nanoparticle. Our findings will help us to better understand the interactions between nanomaterials and cellular signaling pathways, especially when the nanomaterials are used as a drug delivery system.

AUTHOR INFORMATION

Corresponding Author

*Tel.: +86 21 3919 4007. Fax: +86 21 3919 4022. E-mail: sunyanhong@sinap.ac.cn; ztzhong@njau.edu.cn.

Notes

The authors declare no competing financial interest.

ACKNOWLEDGMENTS

This work was supported by the Ministry of Science and Technology of China (2012CB825800, 2012CB932600, 2012CB825805), the National Natural Science Foundation of China (No.11179004, 11275251, U1232113, U1232114, 31170077), K.C.Wong Education Foundation, and Youth Innovation Promotion Association CAS.

REFERENCES

(1) Tsurufuji, S.; Sugio, K.; Takemasa, F. *Nature* **1979**, *280*, 408−410.
(2) Bronicki, R. A.; Backer, C. L.; Baden, H. P.; Mavroudis, C.; Crawford, S. E. *Ann. Thorac. Surg.* **2000**, *69*, 1490−1495.
(3) Benedetti, S.; Pirola, B.; Poliani, P. L.; Cajola, L.; Pollo, B.; Bagnati, R.; Magrassi, L.; Tunici, P.; Finocchiaro, G. *Gene Ther.* **2003**, *10*, 188−192.
(4) Patel, J. A.; Kunimoto, M.; Sim, T.; Chonmaitree, T.; Schmalstieg, F. *Pediatr. Res.* **1994**, *35*, A191.
(5) Londono, P.; Komura, A.; Hara, N.; Zipris, D. *Clin. Immunol.* **2010**, *135*, 401−411.
(6) Schacke, H.; Docke, W. D.; Asadullah, K. *Pharmacol. Ther.* **2002**, *96*, 23−43.
(7) Di Fazano, C. S.; Messica, O.; Quennesson, S. *Rev. Rheumatol. Engl. Ed.* **1999**, *66*, 235.
(8) Dietert, R. R.; Lee, J. E.; Olsen, J. *Toxicology* **2003**, *194*, 163−176.
(9) Mizoguchi, K.; Yuzurihara, M.; Ishige, A. *Psychoneuroendocrino* **2001**, *26*, 443−459.
(10) Wyllie, A. H. *Nature* **1980**, *284*, 555−556.
(11) Helmberg, A.; Auphan, N.; Caelles, C.; Karin, M. *EMBO J.* **1995**, *3*, 452−460.
(12) Pace, T. W.; Hu, F.; Miller, A. H. *Brain, Behav., Immun.* **2007**, *1*, 9−19.
(13) Gao, H. B.; Tong, M. H.; Hu, Y. Q. *Mol. Cell. Endocrinol.* **2003**, *1*, 153−163.
(14) Migliorati, G.; Nicoletti, I.; Crocicchio, F. *Cell. Immunol.* **1992**, *143*, 348−356.
(15) Marchetti, M. C.; Marco, B. D.; Cifone, G. *Blood* **2003**, *101*, 585−593.
(16) Schafer, S. C.; Wallerath, T.; Close, E. I. *Am. J. Physiol.-Heart C* **2005**, *288*, 436−444.
(17) Lai, H. S.; Chen, W. J.; Chiang, L. Y. *World J. Surg.* **2000**, *24*, 450−454.
(18) Simon, H. U.; Haj-yehia, A.; Levi-Schaffer, F. *Apoptosis* **2000**, *5*, 415−418.
(19) Kraaij, M. D.; van der Kooij, S. W.; Reinders, M. E. J.; Koekkoek, K.; Rabelink, T. J.; van Kooten, C.; Gelderman, K. A. *Mol. Immunol.* **2011**, *49*, 549−557.
(20) You, J. M.; Yun, S. J.; Nam, K. N. *Can. J. Physiol. Pharmacol.* **2009**, *87*, 440−447.
(21) Yasushi, O.; Yukiko, K.; Makoto, K. *Muscle Nerve* **2004**, *30*, 49−54.
(22) Heiney, P. A.; Fischer, J. E.; Mcghie, A. R. *Phys. Rev. Lett.* **1991**, *66*, 2911−2914.
(23) Kazuo, N.; Norio, N.; Eiichi, S. *J. Natl. Cancer. Inst.* **2001**, *93*, 1739−1746.
(24) John, D. H.; Efstathios, P.; Marsha, J. M. *J. Clin. Invest.* **1996**, *98*, 1400−1408.
(25) Kovacs, J. J.; Murphy, P. J. M.; Gaillard, S. *Mol. Cell.* **2005**, *5*, 601−607.

(26) Scherrer, L. C.; Dalman, F. C.; Massa, E. *J. Biol. Chem.* **1990**, *35*, 21397−21400.
(27) Brink, M.; Humbel, B. M.; Dekloet, E. R.; Vanderiel, R. *Endocrinology* **1992**, *130*, 3575−3581.
(28) Czar, M. J.; Galigniana, M. D.; Silverstein, A. M.; Pratt, W. B. *Biochemistry* **1997**, *25*, 7776−7785.
(29) Scheinman, R. I.; Gualberto, A.; Jewell, C. M. *Mol. Cell. Biol.* **1995**, *2*, 943−953.
(30) Takeda, T.; Kurachi, H.; Yamamoto, T. *J. Endocrinol.* **1998**, *159*, 323−330.
(31) Tak, P. P.; Firestein, G. S. *J. Clin. Invest.* **2011**, *107*, 7−11.
(32) Kaltschmidt, C.; Kaltschmidt, B.; Lannesvieira, J. *J. Neuroimmunol.* **1994**, *55*, 99−106.
(33) Liu, R. L.; Cai, X. Q.; Wang, J. D.; Li, J. G. *J. Nanosci. Nanotechnol.* **2009**, *5*, 3171−3176.
(34) Ray, A.; Prefontaine, K. E. *Proc. Natl. Acad. Sci.* **1998**, *94*, 557−572.
(35) Ryan, K. M.; Ernst, M. K.; Rice, N. R.; Vousden, K. H. *Nature* **2000**, *404*, 892−897.
(36) Gharbi, N.; Pressac, M.; Hadchouel, M. *Nano. Lett.* **2005**, *12*, 2578−2585.
(37) Cai, X. Q.; Jia, H. Q.; Liu, Z. B. *J. Neurosci. Res.* **2008**, *16*, 3622−3634.
(38) Liu, R. L.; Yin, J. J.; Li, W. X. *Carbon* **2006**, *44*, 387.
(39) Wyllie, A. H.; Morris, R. G. *Am. J. Pathol.* **1982**, *109*, 78−87.
(40) Delfino, D. V.; Spinicelli, S.; Pozzesi, N.; Velardi, E. *Cell. Death Differ.* **2011**, *18*, 183−190.
(41) Heidari, N.; Miller, A. V.; Hicks, M. A. *Cell. Death Dis.* **2012**, *3*, 1−7.
(42) Baulieu, E. E. *Science* **1989**, *4924*, 1351−1357.
(43) Htun, H.; Barsony, J.; Renyi, I. *Proc. Natl. Acad. Sci. U.S.A.* **1996**, *10*, 4845−4850.
(44) Meaney, M. J.; Viau, V.; Aitken, D. H. *Brain Res.* **1988**, *1*, 198−203.
(45) Vacca, A.; felli, M. P.; Farina, A. R. *J. Exp. Med.* **1992**, *3*, 637−646.
(46) McEwan, I.; Wright, A.; Gustafsson, J. A. *BioEssays* **1997**, *2*, 153−160.
(47) Filep, J. G.; Delalandre, A.; Payette, Y. *Circulation* **1997**, *1*, 295−301.
(48) Caius, G. R.; Donghui, C.; Amar, N. *Mol. Cell. Biol.* **2006**, *2*, 668−677.
(49) Yoshioka, J.; Chutkow, W. A.; Lee, S.; Kim, J. B.; Yan, J.; Tian, R.; Lindsey, M. L.; Feener, E. P.; Seidman, C. E.; Seidman, J. G.; Lee, R. T. *J. Clin. Invest.* **2012**, *122*, 267−279.